PHYSICAL REVIEW B
CONDENSED MATTER

THIRD SERIES, VOLUME 46, NUMBER 13 1 OCTOBER 1992-I

Phase diagram of the Frenkel-Kontorova-Devonshire model

S. Little and A. Zangwill
School of Physics, Georgia Institute of Technology, Atlanta, Georgia 30332
(Received 28 February 1992)

We study a generalization of the Frenkel-Kontorova (FK) model where the usual harmonic spring potential between neighboring atoms is replaced by a phenomenological potential identical in form to a sixth-degree Landau free-energy functional proposed by Devonshire. The resulting model is a natural extension of current FK-type models with nonconvex interactions. It also provides a first step toward the construction of a theory of the structure of an epitaxial film that undergoes a first-order phase transition from a high-symmetry phase to a degenerate low-symmetry phase. The phase diagram is obtained as a function of temperature and misfit (for representative choices of the remaining parameters) by use of the effective potential method of Griffiths and Chou. Among other unusual features, we find commensurate phases and soliton structures in which all competing phases are present simultaneously.

I. INTRODUCTION

The Frenkel-Kontorova (FK) model[1] characterizes a one-dimensional chain of harmonically coupled particles subject to an external sinusoidal potential. As such, it is the simplest description of the competition between bulk and interfacial free-energy effects which determines the structure of an epitaxial thin film.[2] More generally, it serves as a prototype for any situation where competing interactions lead to a modulated ground state.[3]

In this paper, we study an extension of this model where the usual quadratic spring potential is replaced by a phenomenological potential identical in form to a sixth-degree Landau free-energy functional introduced by Devonshire[4] in connection with a study of ferroelectricity. As a function of a single parameter (which we shall regard as the temperature), the potential changes smoothly from a quadratic single well to a symmetric triple well and finally to a symmetric double well (Fig. 1). This functional, of course, is a standard model free energy for a material which undergoes a first-order structural phase transition from a nondegenerate high-symmetry state to a degenerate low-symmetry state.[5] By use of the so-called effective potential method of Griffiths and Chou,[6] the exact phase diagram of this model is obtained as a function of temperature and the lattice misfit between the substrate and the chain for several representative choices of the remaining parameters.

Because the spring potential we employ generally is a nonconvex function of the separation between neighboring atoms, our results contribute to the evolving understanding[7] of this class of generalizations of the basic FK model. Our principal motivation, however, comes from real experimental situations where an as-grown film exhibits single-crystal epitaxy with its substrate but then undergoes a first-order structural phase transition as a function of a change in conditions. Examples include temperature-induced transitions in epitaxial films of ferroelectric[8] and high-T_c (Ref. 9) material and film

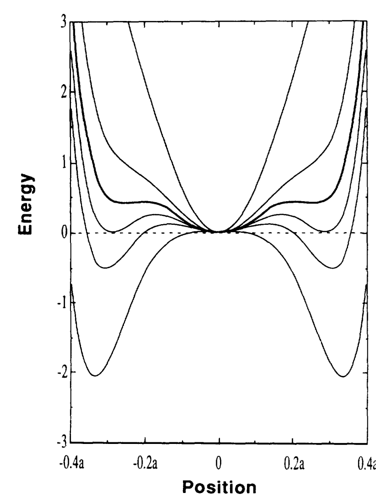

FIG. 1. Evolution of the phenomenological spring potential as a function of the dimensionless energy parameter A_2 in (1). Successive curves from top to bottom correspond to progressively lower temperature. The two substrates discussed in the text have well depths of 0.14 and 0.4 in the scale of the vertical axis.

thickness-induced transitions in systems, e.g., α-Sn/CdTe,[10] where the overlayer is epitaxially stabilized in a bulk-unstable (or metastable) structure. Although the Devonshire free energy is not strictly applicable to, say, a pure cubic-to-tetragonal structural transition (the presence of a cubic invariant drives the transition first order in that case[11]), we adopt the point of view advocated by Falk[12] and others[13] whereby the essential point is the possible coexistence of the high- and low-temperature phases.

This fact is important because a common feature of all the experiments noted above is that the transformed system is still epitaxial but no longer single crystalline. Instead, a characteristic *twinned* morphology is observed. Such a result is expected on the basis of macroscopic elasticity calculations[14,15] and may be understood as a mechanism of epitaxial strain relief. In the context of the related problem of bulk martensitic phase transformations, twinning of this kind was studied in an approximate way by Marianer and Bishop[16] with a double-well version of the FK model. As expected, we recover some of their results in the appropriate (low-temperature) limit of our model. On the other hand, our exact numerical approach permits us to study the competition between this form of strain relief and the mechanism of misfit dislocation (soliton) generation familiar from the standard FK model.

II. THE MODEL

The generalized FK model considered in this paper is defined by the potential energy

$$H=\sum_{n=-\infty}^{\infty}\left[A_2(x_{n+1}-x_n-\gamma)^2-A_4(x_{n+1}-x_n-\gamma)^4+A_6(x_{n+1}-x_n-\gamma)^6+V(1-\cos 2\pi x_n)\right]. \tag{1}$$

Here, x_n is the position of the nth atom and γ is the lattice constant of the presumed high-temperature "cubic" phase of the film material. Both are measured in units of the substrate lattice constant so that the quantity $1-\gamma$ is seen to be identical with the conventional definition of lattice misfit.[2,3] The energy parameter V measures the strength of the substrate potential while A_2 is imagined to be a linear function of $T-T_c$. A_4 and A_6 are fixed positive constants. The anharmonic spring potential thus fixes three lengths: a particle in the middle (M) well of the spring potential denotes a unit cell of the film with a lattice constant equal to that of the high-temperature "cubic" phase, while a particle in the left (L) or right (R) well of the spring potential denotes a unit cell of the film with a lattice constant equal to, respectively, the shorter or longer lattice constant of the low-temperature "tetragonal" phase. This denotation will be used consistently below, although, of course, the substrate induces inhomogeneous strains into the chain.

Since the absolute scale of energy is immaterial, the model as defined has four free parameters. Even so, the parameter space is still too large for practical study by our methods. Hence, in what follows, we present the phase diagram in rather great detail as a function of misfit (γ) and temperature (A_2) for four choices of the remaining two parameters. We focus on a wide well spring potential where the magnitude of the tetragonal distortion is about $0.3a$ and a narrow well spring potential where the magnitude of this distortion is about $0.03a$. The ratio A_4^3/A_6^2 is held fixed in order to guarantee that the same interwell energy barrier obtains in the two cases. Two values of the substrate potential strength are examined as well: a strongly corrugated case where V is 30% greater than the energy barrier between wells at T_c and a weakly corrugated case where V is 30% less than this energy barrier. Due to the symmetry of the spring potential, it is sufficient in every case to choose the range of γ from a maximum value of unity (where the high-temperature M phase is lattice matched to the substrate) to a minimum value just below the point where the low-temperature R phase is so lattice matched. We focus on a temperature range within about 25% of T_c since the high-[3] and low-temperature[16] limits are well understood.

The phase diagram is obtained by use of the effective potential method of Griffiths and Chou[6] with the numerical implementation suggested by Floria and Griffiths.[17] The method is exact in the sense that it seeks the absolute minimum of the potential energy rather than merely identifying extrema of the energy as in other approaches to this problem. The efficacy of the method is determined entirely by the choice one makes for the discretization of the spatial continuum available to the variables x_n. More precisely, one chooses a grid of N points per interval of length a. The now-discrete model based on (1) is solved by a systematic search for the cycle of N atoms or less with the lowest total energy. It is important to note that the solution one obtains is periodic although the physical length of the period (cycle) along the substrate is not fixed *a priori*.

Typically we chose $N=1000$, although at selected spots much larger values were used to confirm the ground state. Such checks occasionally produced minor cycle length changes although the ground-state configuration was always qualitatively unchanged. As noted by Floria and Griffiths,[17] convergence generally is slower when the ground-state cycle length increases or there are nearly degenerate states near the ground state. In these situations we found that values of N as large as 10^4 were required to ensure accurate results.

The nature of the solution is encoded in the phase variable ϕ_n defined as the deviation of the position of the nth atom from the nth substrate minimum:

$$x_n=na+\phi_n a\ . \tag{2}$$

Figure 2 illustrates this quantity for an 11-atom cycle. To determine the detailed structure of the film, i.e., whether each unit cell is associated with the "cubic" or one of the "tetragonal" phases, one simply compares the slope of each segment of this curve to the slopes of the lines which correspond to ϕ_n for each of the three purely incommensurate phases: M, L, or R. For this example, one finds that the cycle is $LRLRMMMMMRLR$ or $(2LR)(4M)RLR$, in a simplified notation to be used

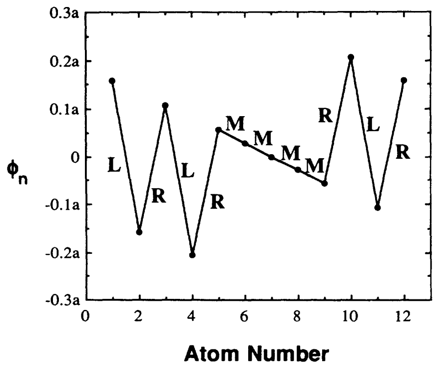

FIG. 2. Phase plot for the 11-atom cycle $(2LR)(4M)RLR$.

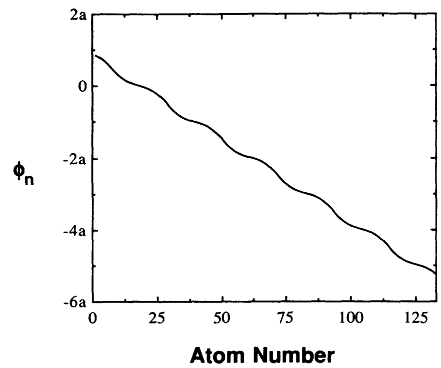

FIG. 4. Phase plot for an incommensurate M ground-state cycle.

henceforth. The fact that ϕ_n has exactly the same value at the beginning and end of the cycle indicates that there is one-to-one correspondence between the particles of the chain and the wells of the substrate.

III. RESULTS AND DISCUSSION

Figure 3 illustrates the temperature-misfit phase diagram for a system with the weakly corrugated substrate potential and the wide well springs defined above. At high temperature, we observe the conventional FK transition from a commensurate M phase to an incommensurate M (IM) phase as a function of increasing misfit (decreasing γ). A plot of ϕ_n at a representative point in the incommensurate phase (Fig. 4) makes clear that the one-to-one correspondence between the chain particles and the substrate wells discussed above is lost by the insertion of an extra atom every 22 substrate wells at this value of the misfit ($\gamma=0.945$). Following conventional terminology,[3] we refer to these defects as solitons. Actually, Fig. 4 corresponds to a temperature just *below* the point marked P in Fig. 3 so that a small increase in γ drives one not into the pure M phase but instead horizontally across a phase boundary into a phase denoted M/R.

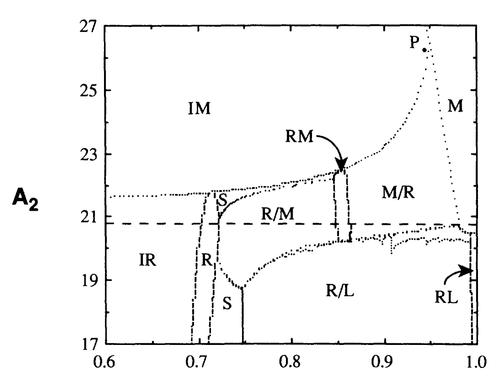

FIG. 3. Global phase diagram for the case of the wide well spring potential and weakly corrugated substrate potential. The horizontal dashed line marks the value of A_2 where the M phase is degenerate with the L and R phases, i.e., $T=T_c$. The lattice misfit is equal to $1-\gamma$. See text for further discussion.

To illustrate this point, Fig. 5 shows the phase plot for the ground-state cycle $R(19M)$, which occurs at the same temperature as the cycle in Fig. 4 but with $\gamma=0.950$. This structure contains no solitons. Indeed, there are no solitons present anywhere within the M/R phase field. Instead, the lattice misfit is accommodated by the insertion of a periodic array of R unit cells embedded in an otherwise pure M phase. To understand this, one need only read the vertical axis of Fig. 5. There, we observe the atoms associated with the majority M phase "walking across" the bottom of the substrate wells until an R defect is inserted. The latter abruptly moves the next atom to the same height on the opposite side of its substrate well. The majority phase then continues until the cycle completes. It is remarkable that R defects are used for this purpose since (as may be seen from the corresponding spring potential curve drawn as a heavy line in Fig. 1) they each cost an amount of energy greatly in excess of the total substrate well depth. Presumably, the net cost to employ solitons is even greater.

The density of R defects in the M/R phase increases as γ decreases. Ultimately, the ground-state cycles are best described as M defects within a majority R phase. This R/M phase persists as the misfit increases further until the pure R phase locks in at a value of γ somewhat larger than that required to exactly match the R phase lattice constant to that of the substrate. It is interesting to note that the domain of absolute stability for the R phase per-

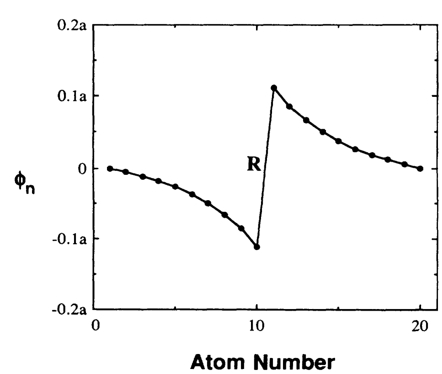

FIG. 5. Phase plot for the 20-atom cycle $R(19M)$.

sists to a temperature well above the bulk transition temperature back to M. This is a simple example of the phenomenon of *epitaxial stabilization* of a bulk unstable (metastable) phase.[15] In real materials, this occurs only in thin films where the interfacial energy is competitive with the condensation energy in the bulk of the film. For the monolayer problem studied here, the effect is quite substantial.

As the misfit is increased still further, the R phase becomes unstable with respect to soliton generation. Just as for the case of the M-IM phase transition, this occurs when the R phase lattice constant shrinks to the point where it is no longer energetically favorable to strain to match the substrate. However, the solitons are of a very different character than in the M phase case. More precisely, the strain accommodation typically is accomplished by the insertion of *several* unit cells of the *other* phases. Thus, one finds, e.g., MMM-type solitons [Fig. 6(a)] at high temperatures near the phase boundary with the IM phase. Indeed, the transition from IM to this incommensurate R (IR) phase may well be continuous. Finally, at the lowest temperatures, the solitons of the IR phase convert to LL-type since the cost of an M-phase unit cell becomes prohibitive.

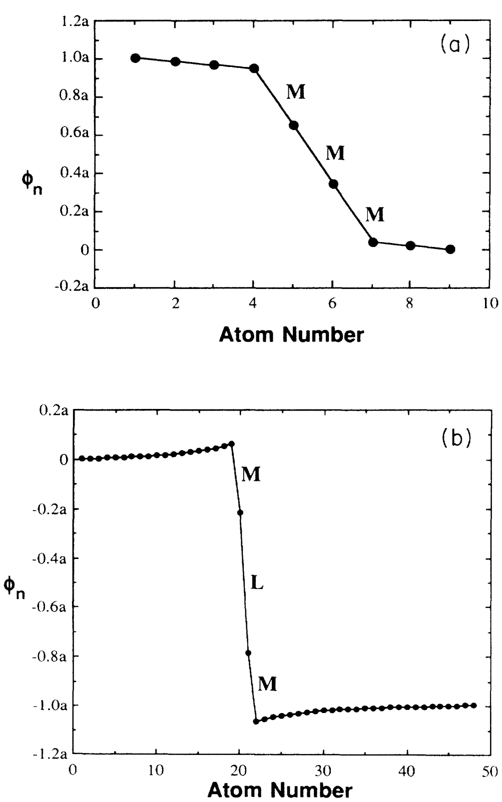

FIG. 6. Phase plot for a ground-state cycle which contains (a) an MMM soliton in a region where the R phase lattice constant is *less* than the substrate lattice constant and (b) an MLM soliton in a region where the R phase lattice constant is *greater* than the substrate lattice constant. The text refers to the latter as an "accidental" soliton. Note that, in both cases, every majority R phase atom resides very near the bottom of a substrate well.

Given the foregoing, the entire low-temperature portion of Fig. 3 is easy to understand. Suppose we begin in the R phase. As the misfit decreases, L defects appear periodically (R/L phase) to relieve the strain. In complete analogy to the discussion of the M/R phase, the defect density increases until, as $\gamma \to 1$, one obtains pure RL. This is almost obvious because, by construction, the length of an RL "microtwin" is equal to the length of two unit cells of M phase.

Evidently, we could refer to each distinct cycle within the R/L, M/R, and R/M phase fields as a "phase" in its own right and search for the corresponding "phase" boundaries. This is the strategy employed in analyses of *ANNI*-type models.[1] Except for the designation of the RM phase, we do not pursue this line of investigation here (nor have we attempted to determine whether the various phase boundaries in Fig. 3 correspond to first-order or continuous phase transitions) because of our future interest in a more realistic model of epitaxy which takes account of domain-wall contributions to the total energy. The strain gradient terms required to do so[16] may be expected to radically alter the microtwin character of the aforementioned "phases" and perhaps the global topology of the phase diagram as well.

We turn now to two rather unusual features of Fig. 3. First, observe that there are two small regions of the phase diagram (denoted "S") where solitons appear even though the length of an R unit cell renders the insertion of extra atoms unnecessary. In the upper region, the solitons are of the MLM variety [Fig. 6(b)] while in the lower region one finds MM and (kL)—where k is an integer—solitons. The source of this phenomenon is that the length of each of these defects is very nearly equal to a multiple of the substrate wavelength in this range of misfit. By this artifice, the system accommodates almost all the misfit within the soliton so that each majority R unit cell can remain near the bottom of its substrate well. It is worth noting that both soliton types place atoms near maxima of the substrate potential. This explains why they disappear in the immediate vicinity of T_c: the insertion of an extra L (M) atom to form an LL (MLM) soliton then produces no spring energy benefit.

The second atypical feature of this phase diagram appears between the M/R and R/L phase fields. We find a region of commensurate states where M, R, and L unit cells appear in the ground-state cycles simultaneously. As revealed in Fig. 7, this LMR region has a very complex shape and most resembles an archipelago. Moreover, each "island" displays an odd-shaped boundary. Consider the island which abuts the M phase. A cycle like $MMRLR$ is typical of those that occur near the rather smooth upper phase boundary. When the temperature is raised so that the phase boundary is crossed, the ground state adjusts to $MMMMR$. This is another example of the replacement of RL by MM as discussed earlier. Upon reducing the temperature, the $MMRLR$ cycle is stable until the lower phase boundary is crossed and an R/L-type cycle is obtained. But it turns out that this simple behavior arises only because the total vertical extent of the LMR phase field is rather narrow at this value of misfit ($\gamma=0.9425$). If, instead, we choose a point where the phase field is very wide, e.g., a value of misfit like $\gamma=0.9075$, which is coincident with one of the narrow peninsulas of the island, a considerable change in the ground-state cycle is observed as the peninsula is traversed from top to bottom. Generally speaking, the original M content of the cycle decreases and the relative number and distribution of R and L unit cells varies until they approach that found in the corresponding R/L cycle across the lower phase boundary.

The LMR phase field contains cycles of extraordinary complexity. For example, well below the upper phase boundary, most of the ground states may be characterized as a background R phase within which are embedded both a periodic array of L defects and a second periodic array of M defects. This behavior may be understood either by careful study of the associated ϕ_n diagrams or from general discussions of the effective interaction between such defects.[3] Occasionally, however, we observe cycles such as

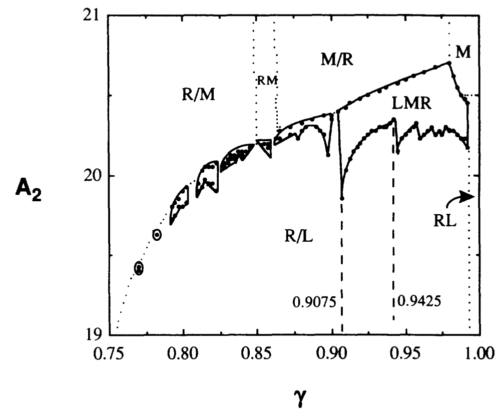

FIG. 7. Blowup of the global phase diagram in the vicinity of the boundary between the M/R and R/L phase fields. Ground-state cycles at two values of γ (indicated by vertical dashed lines) are discussed in the text. The lattice misfit is equal to $1-\gamma$.

$$(2LRRR)LRR\,(5LRRR)LRR\,(5LRRR)LRR\,(2LRRR)(2LRRMRR)\,,$$

where the M defects are *not* symmetrically arranged. The extreme sensitivity of the ground-state cycle to misfit can be judged from the fact that the long peninsula of complex phases discussed above is bounded (towards lower γ) by a pronounced gap where the R/L phase field directly adjoins the M/R phase field. The ground-state cycle within this gap is simply LRR. Our model thus conforms to the general observation[3] that short period cycles exhibit relatively greater stability intervals than long period cycles.

At this point, it is appropriate to ask whether the phase diagram of Fig. 3 is robust. That is, which features survive variations in the parameters of the model and which do not? As noted earlier, we have studied three other choices of spring-substrate parameters. In all cases, the phase diagram is qualitatively similar to Fig. 3 except for the "S" regions. For example, the vertical extent of the LMR archipelago shrinks considerably for the narrow well case but does not disappear. However, the "unnecessary" solitons are observed to vanish if either the substrate adhesion becomes too strong or the tetragonal distortion of the film becomes too small. This is not difficult to rationalize given our earlier account of the origin of these structures.

A final, interesting result of this survey concerns the fate of the microtwin structures found in both the commensurate and incommensurate portions of Fig. 3. For the "narrow-well" case, these objects still inhabit the R/M, M/R, and R/L commensurate phase fields but disappear from the IR phase. Instead, the IR solitons are extended and generally have the form $(pM)(qL)(pM)$, where p and q are integers. The maximum values of p and q scale inversely with the magnitude of the tetragonal distortion. Moreover, the ratio p/q increases steadily as one heats the IR phase. We suspect that these extended solitons may be amenable to study by analytic means.

IV. SUMMARY AND CONCLUSION

We have introduced and investigated a nonconvex extension of the Frenkel-Kontorova model where the usual harmonic spring potential is replaced by a sixth-degree polynomial in the interparticle spacings. The latter was chosen to serve as a model for the free energy of a film which undergoes a first-order transition from a high-temperature "cubic" phase to a low-temperature "tetragonal" phase. The usual subtle interplay between the substrate and spring potentials characteristic of the conventional FK model is enriched by the presence of *four* competing lengths: the substrate periodicity, the length of the "cubic" unit cell, and the long and short lengths of the "tetragonal" unit cell. An exact numerical algorithm was used to obtain the phase diagram as a function of temperature and lattice misfit for representative values of the other model parameters. In addition to the homogeneous lattice-matched bulk phases, we find (i) epitaxial stabilization of a bulk metastable phase, (ii) simple commensurate phases where a periodic array of microtwins disrupts otherwise homogeneous structures, (iii) an archipelago-shaped commensurate phase field where unit cells of all three structural species are present simultaneously, and (iv) incommensurate phases where both conventional and unconventional solitons provide misfit accommodation.

In subsequent papers, we plan to report generalizations of the work presented here which more nearly approximate the situation in real epitaxial films. These studies, currently in progress, involve the addition of a strain gradient term to the potential energy[16] and the coupling of multiple FK chains together to form a thin film.[18]

ACKNOWLEDGMENTS

The authors gratefully acknowledge stimulating discussions with our colleague Ahmet Erbil and the support of the U.S. Department of Energy under Grant No. FG05-88ER45369. S.L. acknowledges financial support from the Tennessee Valley Chapter of the American Vacuum Society.

[1]J. Frenkel and T. Kontorova, J. Phys. USSR **1**, 137 (1939).
[2]I. Markov and S. Stoyanov, Contemp. Phys. **28**, 267 (1987).
[3]See, e.g., R. B. Griffiths, in *Fundamental Problems in Statistical Mechanics VII,* edited by H. van Beijeren (Elsevier, Amsterdam, 1990), pp. 69–110.
[4]A. F. Devonshire, Adv. Phys. **3**, 86 (1954).
[5]See, e.g., J.-C. Tolédano and P. Tolédano, *The Landau Theory of Phase Transitions* (World Scientific, Singapore, 1987), Chap. 4.
[6]R. B. Griffiths and W. Chou, Phys. Rev. Lett. **56**, 1929 (1986).
[7]M. Marchand, K. Hood, and A. Caillé, Phys. Rev. B **37**, 1898 (1988).
[8]B. S. Kwak, A. Erbil, B. J. Wilkens, J. D. Budai, M. F. Chisholm, and L. A. Boatner, Phys. Rev. Lett. **68**, 3733 (1992).
[9]J. D. Budai, R. Feenstra, and L. A. Boatner, Phys. Rev. B **39**, 12 355 (1989).
[10]J. L. Reno and L. L. Stephenson, J. Electron. Mater. **19**, 549 (1990).
[11]Yu. A. Izyumov, V. M. Laptev, and V. N. Syromyatnikov, Fiz. Tverd. Tela (Leningrad) **30**, 1623 (1988) [Sov. Phys. Solid State **30**, 938 (1988)].
[12]F. Falk, Acta Metall. **28**, 1773 (1980).
[13]S. Kartha, T. Castán, J. A. Krumhansl, and J. P. Sethna, Phys. Rev. Lett. **67**, 3630 (1991).
[14]A. L. Roitburd, Phys. Status Solidi A **37**, 329 (1976); A. L. Roitburd, in *Heteroepitaxy of Dissimilar Materials,* edited by R. F. C. Farrow, J. P. Harbison, P. S. Peercy, and A. Zangwill (Materials Research Society, Pittsburgh, 1991), pp. 255–268.
[15]R. Bruinsma and A. Zangwill, J. Phys. (Paris) **47**, 2055 (1986).
[16]S. Marianer and A. R. Bishop, Phys. Rev. B **37**, 9893 (1988).
[17]L. M. Floria and R. B. Griffiths, Numer. Math. **55**, 565 (1989).
[18]E. Granato, J. M. Kosterliz, and S. C. Ying, Phys. Rev. B **39**, 3185 (1989).